Testing a pneumatic underwater glider in shallow water

Artur Wolek, Tejaswi Gode, and Craig A. Woolsey
Department of Aerospace and Ocean Engineering
Virginia Tech
Blacksburg, VA 24060

Jake Quenzer and Kristi A. Morgansen
Department of Aeronautics and Astronautics
University of Washington
Seattle, WA 98195

***Abstract*—In this paper we discuss the testing of a novel underwater glider designed to be fast and maneuverable for operation in the littorals. The glider's pneumatic buoyancy engine was shown to operate reliably and provide large, rapid displacements. However, the compressibility of the bladder and associated change in tank weight (from exhausting air with each dive) presented significant challenges in trimming the vehicle. Several design considerations unique to a glider with unlimited roll control (and a cylindrical moving mass actuator) were identified through testing. The performance of a long baseline acoustic positioning system was characterized, and the challenges associated with deploying this system in a shallow-water, rocky-bottom lake are discussed.**

I. Introduction

Underwater gliders are robust and long endurance ocean sampling platforms that are increasingly being deployed in coastal regions. This new environment is characterized by shallow waters and significant currents that can challenge the mobility of these efficient (but traditionally deep diving and slow moving) vehicles. Since gliders have no external moving parts they are resistant to biofouling and are well suited for long-endurance missions in the littorals. However, to overcome the challenges associated with shallow waters and significant currents, there is a need to further improve glider performance. Performance improvements may be achieved by advancing platform technologies (e.g., actuator capabilities, hydrodynamics, and energy storage) and/or by developing improved motion planning strategies. Recently, a number of novel motion planning strategies have been developed to improve glider performance on the *micro-scale* (i.e., on the scale of a few turn radii of the vehicle). These strategies may be used to enhance robustness in currents [1], minimize transit time [2], or maximize efficiency [3]. Our goal was to validate such planning strategies experimentally. We considered using commercially available gliders, however the limited access to their proprietary software and control systems prohibited this option. Instead, we designed our own open-source vehicle – the *Virginia Tech Underwater Glider* (*VTUG*), shown in Fig. 1(a). The *VTUG* is designed specifically for shallow water operations and utilizes a pneumatic buoyancy engine for depth rate control. A cylindrical (rotating and translating) moving mass is used for attitude control. The design of the *VTUG* is described in [4]. In this paper, we discuss the performance of the *VTUG* and the successes and challenges that we experienced in testing this novel glider concept. We also describe the design and testing of an acoustic long-baseline (LBL) ranging system developed to provide position estimates of the glider while it is underway. The LBL system consisted of a series of GPS-equipped buoys/beacons deployed in a shallow lake as shown in Fig. 1(b).

This paper is organized as follows. Section II describes the performance of the pneumatic buoyancy engine. Section III discusses the performance of the attitude control mechanism and lessons learned while trimming the vehicle. Section IV summarizes the design and testing of the LBL system. Section V reviews the results from sawtooth glide experiments. Section VI gives our conclusions.

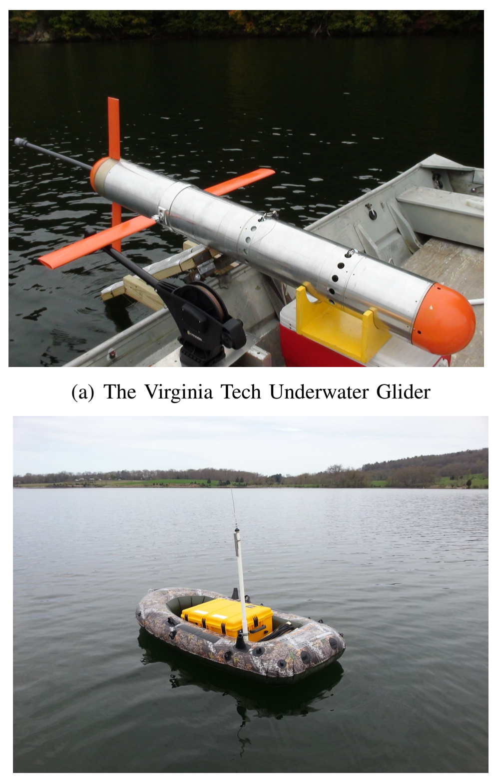

(a) The Virginia Tech Underwater Glider

(b) Acoustic buoy deployed on a raft as part of a long baseline acoustic positioning and communication system

Fig. 1: Testing at Claytor Lake, VA

978-0-933957-43-5 ©2015 MTS

II. Pneumatic Buoyancy Engine Performance

The pneumatic buoyancy engine of the *VTUG* consists of a scuba tank and a series of solenoid flow control valves and pressure sensors that regulate the pressure (and hence buoyancy) of an elastomeric bladder. Here, we develop a basic model of this buoyancy engine that illustrates the performance of this design under various operating conditions, and its open loop response to changes in depth. Let the total buoyancy of the glider be $B = B_{\mathrm{RB}} + B_{\mathrm{BE}}$, where B_{RB} is the rigid body buoyancy (for shallow waters we may neglect hull compressibility, and assume this quantity is fixed), and where B_{BE} is the variable buoyancy generated by the buoyancy engine. For a glider with "dry weight" $W = mg$ (where m is the glider's mass and g is gravitational acceleration), the net force on the glider is referred to as the net weight $\tilde{W} = W - B$. In the following analysis, we assume that the glider is neutrally buoyant ($\tilde{W} = 0$) when $B_{\mathrm{BE}} = 5.5$ lbs (a displacement of 2.5 L of water). Since the working fluid in the bladder (air) is compressible, the endurance of the glider is a function of the operating depth. The bladder reaches an equilibrium volume when the ambient pressure p_{amb} and elastic bladder pressure p_{blad} is balanced by the internal bladder pressure p_{int}:

$$p_{\mathrm{amb}} + p_{\mathrm{blad}} - p_{\mathrm{int}} = 0\,. \qquad (1)$$

The ambient pressure is given by the hydrostatic equation $p_{\mathrm{amb}} = p_{\mathrm{atm}} + \rho_{\mathrm{H2O}} g z$ where p_{atm} is the atmospheric pressure, z is the depth, and ρ_{H2O} is the density of water. Assume that the elastic pressure p_{blad} depends only on the volume $V\!\!\!/$ of the stretched bladder. This relationship (see Fig. 2) was experimentally determined by submerging the buoyancy engine in a container and measuring the weight of water displaced by the bladder (as it overflowed through a hole in the container wall onto a scale) with changes in p_{blad}. The internal bladder pressure is given by the ideal gas law

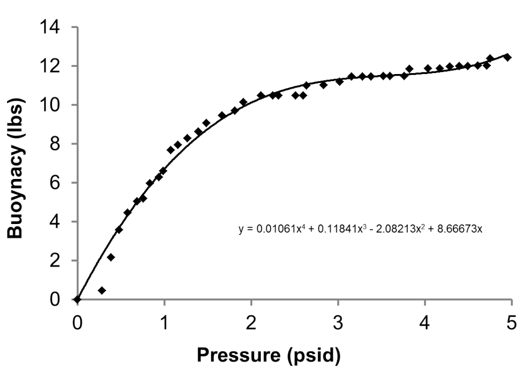

Fig. 2: Experimental bladder pressure vs. buoyancy curve

$p_{\mathrm{int}} = nRT/V\!\!\!/$ where n is the number of moles of air in the bladder, R is the ideal gas constant, and T is the temperature. Then the equilibrium condition (1) is rewritten as

$$p_{\mathrm{atm}} + \rho_{\mathrm{H2O}} g z + p_{\mathrm{blad}}(V\!\!\!/) - \frac{nRT}{V\!\!\!/} = 0\,. \qquad (2)$$

Using (2) we may determine the amount of air n_{cycle} required to inflate the bladder at a given depth and volume. The amount of air available n_{tank} in a scuba tank with a known volume and pressure can also be easily computed. (*VTUG*'s scuba tank has a maximum pressure $p_{\mathrm{tank}} = 3,442$ psi and corresponding volume $V\!\!\!/_{\mathrm{tank}} = 183$ in^3.) An upper bound on number of available dives for a given scuba tank is then $N = n_{\mathrm{tank}}/n_{\mathrm{cycle}}$. (This assumes no losses and that the bladder is inflated only once at depth and exhausted fully on the surface after each dive cycle.) Contours of fixed N are shown in Fig. 3 for various bladder displacements and depths. At the most extreme design point, of 5 L displacement and 100 m depth, we expect an endurance of at most 13 dives. At shallower depths many more dives can be expected. Replacing the scuba tank in the field can further extend the endurance.

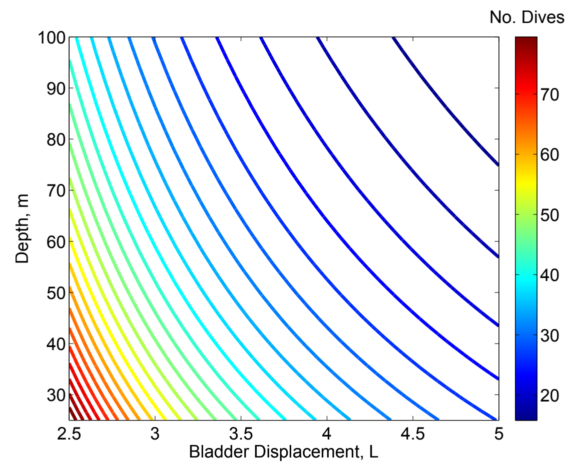

Fig. 3: Number of dives

Since the air-filled bladder is compressible, ambient pressure changes with depth cause the bladder to expand during ascents and compress during descents. To compensate for this the bladder pressure (and hence volume) is regulated using two valves which we refer to as the inflator (to inject air into the bladder) and deflator (to exhaust air to the hydrosphere). The open loop response of the bladder with a fixed amount of air subject to changes in depth is given in Fig. 4. We use the term "open loop" loosely here to refer to the set of equilibrium bladder displacements/volumes for a fixed amount of air n. (Rather than the dynamic response of the bladder to changes in depth.)

As mentioned previously, we assume that the glider is neutrally buoyant at 2.5 L bladder displacement. Thus if the bladder is at a volume > 2.5 L, the glider will ascend and the bladder equilibrium volume will follow a particular contour given in Fig. 4 that corresponds to the amount of air at the initial volume and depth. Similarly, if the bladder volume is initially < 2.5 L then the glider will descend, again the volume will follow the corresponding contour in Fig. 4. It is clear that the bladder displacement is sensitive to changes in depth and that different initial volumes can have entirely different "open loop" responses.

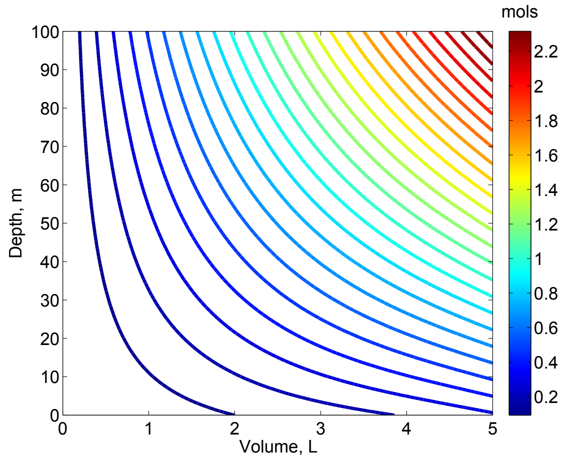

Fig. 4: Bladder open loop response

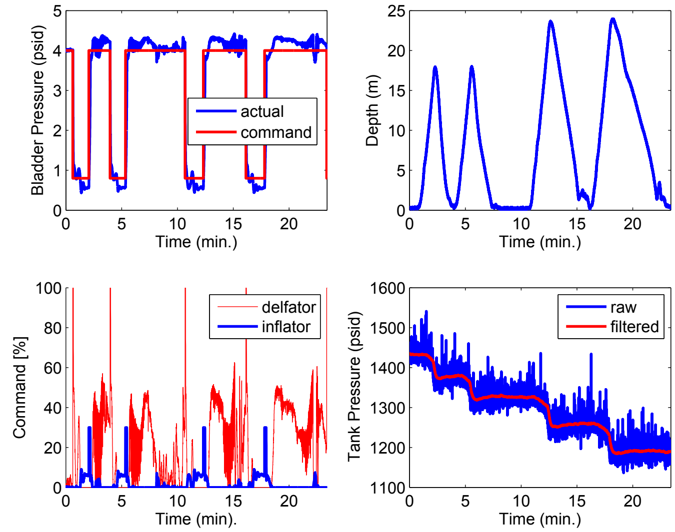

Fig. 5: Buoyancy engine tests at Claytor Lake, VA

Extensive testing of the buoyancy engine in Claytor Lake, VA demonstrated the feasibility of this pneumatic design. Figure 5 shows a series of dives to target depths of 15 m, then to 20 m, with corresponding changes in bladder pressure, depth, actuator commands and tank pressure.

Since the pneumatic buoyancy engine is an open system (exhausting air with each dive) the vehicle becomes lighter as the tank is depleted. To minimize the changes in trim, the tank CG was designed to be as close as possible to the vehicle's CG. However, since the weight of the air in the tank at full pressure is about 2 lbs even small errors in the estimates of these CG locations could cause large changes in trim. The change in tank weight may cause the CG of the vehicle to change in both the longitudinal and vertical direction (i.e. the change in CG may affect both the stability of the vehicle as well as the equilibrium pitch attitude). In practice, we found this change in trim was significant and difficult to accomodate for – any gain tuning or trimming of the vehicle was only valid for a few dives, after which the vehicle had a drastically different nominal pitch attitude, bladder pressure response, and depth rate. This made the trimming process challenging and prevented us from achieving our desired performance requirements for the glider.

Future glider designs may mitigate some of the challenges described herein by using a higher pressure bladder that is less sensitive to changes in depth. Further, an improved control strategy may be employed that accurately models and accounts for the changes in trim. For example, feed-forward commands may be used to adjust the nominal position of the moving mass with tank pressure, or an adaptive control law may be derived to compensate for slowly varying parameters in the system.

III. Attitude Control and Trimming

The goal of trimming the glider is to achieve a desired weight, buoyancy, and balance that meets some performance and stability requirements. This requires carefully designing the vehicle and actuators to accommodate a range of center of buoyancy (CB) and center of gravity (CG) positions. The glider must be trimmed for a number of operating conditions: a range of desired depth rates and pitch attitudes during ascents and descents, the surface communication stance (where the tail sticks above the water to improve radio and Global Positioning System (GPS) reception), and the ability to roll completely around with one revolution of the moving mass. These are often competing objectives for which the trade-off must be well understood to successfully trim the vehicle.

A. Pitch Trimming

A free body diagram of the forces acting on a glider at a fixed pitch angle are shown in Fig. 6. (Note that the hydrodynamic lift and drag forces are neglected for simplicity.) It is assumed that all of the forces act along the vehicle centerline, with the exception of the moving mass weight W_{MM} which we assume acts a distance z_{MM} below the centerline. The attainable pitch angles will change with the buoyancy generated by the buoyancy engine B_{BE}, and the weight of the tank W_{T}. The remaining weight of the rigid body (excluding W_{MM} and W_{T}) is denoted W_{RB} so that $W = W_{\mathrm{RB}} + W_{\mathrm{T}} + W_{\mathrm{MM}}$. The total buoyancy is $B = B_{\mathrm{RB}} + B_{\mathrm{BE}}$. The longitudinal location through which each force acts is measured from the back of the vehicle (indicated by l in Fig. 6).

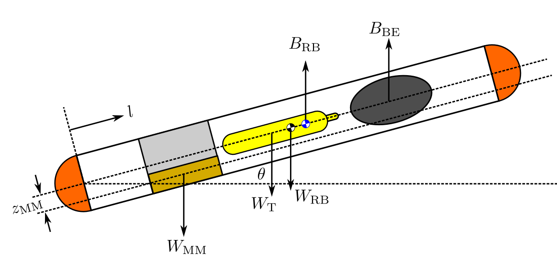

Fig. 6: Forces in pitch

Summing the moments about a reference point in Fig. 6 and equating them to zero gives a condition for the equilibrium pitch attitude. By adjusting the moving mass position, tank weight, and bladder buoyancy parameters, one may determine if the vehicle is capable of meeting the desired range pitch attitudes. Inevitably the mass properties of the manufactured vehicle will deviate from those assumed during the design. Uncertainty analysis must be incorporated into the design process, and trim adjustments must be made by installing ballast (e.g. lead) or buoyancy (e.g. syntactic foam) onto the vehicle as needed. Although we conducted this careful analysis described above, we encountered several challenges in trimming the glider's pitch attitude that we did not anticipate during the design phase. Deep diving gliders that move slowly in the open ocean are not constrained by the time it takes to establish a steady glide and can neglect actuator dynamics. However, shallow water gliders must have actuators that are fast enough such that the steady glide is established quickly. Our slow translational moving mass actuator made it difficult to establish a steady glide in the 25 m of depth at our testing site. We also found that the glider's pitch attitude was sensitive to changes in trim (e.g. small changes in moving mass position, tank weight, or even trapped air bubbles affected the pitch attitude drastically). Although this pitch sensitivity made the glider highly maneuverable, it also made it difficult to control and tune for satisfactory glide performance. The reason for this pitch sensitivity is, in part, because a glider designed to roll completely is inherently less stable than a conventional glider with limited roll capabilities (with an equally heavy moving mass). The rigid body weight of a glider that "flips over" should not contribute to the vehicle's "bottom-heaviness" if the roll dynamics are to be equivalent in both an upright and inverted orientation. (This point will be explained in detail in Section III-C.) The bottom-heaviness of the vehicle affects the stability of the vehicle both in roll and in pitch. See [5], [6] for a detailed discussion of the effect of bottom-heaviness on the longitudinal stability of a steady glide.

Our testing experiences highlight the need to carefully consider the actuator dynamics and time to establish a steady glide in shallow underwater glider design. Further, the analysis of the attainable range of pitch attitudes should also include a study of the sensitivity to disturbances and small changes in trim at each desired equilibrium pitch attitude.

B. Communication Stance Trimming

The communication stance (see Fig. 7) is used to extend the tail above the water and improve GPS and radio reception. This desired attitude suggests making the glider nose-heavy (i.e. moving the internal mass forward) and as buoyant as possible (so that more of the tail is exposed). However, because the bladder is located near the front of the vehicle, increases in buoyancy tend to pitch the nose up and reduce the angle of the tail. Thus, there is a trade-off between these two objectives. Determining the surface communication pitch attitude for a given bladder buoyancy, tank weight, and moving mass position is particularly challenging because one must account for the change in the CB and B_{RB} when the vehicle is partially exposed to the air.

Fig. 7: Glider in a communications stance

If the moving mass alone does not pitch the vehicle down adequately, then buoyancy foam and ballast weight must be re-distributed such that the nose is heavier and the tail is more buoyant. While this may improve the communications stance, it will bias the range of attainable pitch attitudes towards steeper nose-down angles. Through testing with the *VTUG*, we found that the best communications stance was achieved when the vehicle was just slightly positively buoyant.

C. Roll Trimming

In the following we compare the properties of a glider designed with unlimited roll control (and a cylindrical moving mass actuator) to that of a traditional glider with limited roll control (and a rectilinear moving mass actuator). This comparison will help underscore some key differences in these respective designs. Consider the orientation of a two-dimensional disk, representing the cross-section of the glider, subject to the forces W_{RB}, W_{MM} and B_{RB} as shown in Fig. 8. For the purposes of this example, we neglect the tank weight and assume the disk is neutrally buoyant with $B_{\mathrm{RB}} - W_{\mathrm{RB}} - W_{\mathrm{MM}} = 0$. Assume that buoyancy acts at the center of the disk. Let a clockwise rotation be denoted by the angle ϕ (the roll angle). Then there are two torques about the center: the torque from the weight of the rigid body $\tau_{\mathrm{RB}} = -\sin\phi W_{\mathrm{RB}} z_{\mathrm{RB}}$, and the torque from the weight of the moving mass τ_{MM}. The motion of the disk is given by $\tau_{\mathrm{RB}} + \tau_{\mathrm{MM}} = I\ddot{\phi}$, where I is the inertia.

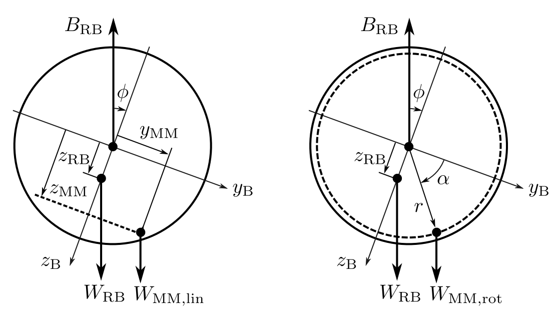

(a) Rectilinear moving mass (b) Cylindrical moving mass

Fig. 8: Forces related to the rolling motion of a glider

First, consider a linear moving mass actuator design. The moving mass position, expressed in the body frame $(y_{\rm B}, z_{\rm B})$, is given by $(y_{\rm MM}, z_{\rm MM})$. We assume that $z_{\rm MM} > 0$ is fixed, whereas $y_{\rm MM} \in [-\bar{y}_{\rm MM}, \bar{y}_{\rm MM}]$ can vary. The torque from the moving mass is then $\tau_{\rm MM} = (y_{\rm MM}\cos\phi - z_{\rm MM}\sin\phi)W_{\rm MM}$. At equilibrium $\ddot{\phi} = 0$, and for a given $y_{\rm MM}$ the equilibrium roll angle is:

$$\phi = \left(\frac{y_{\rm MM}W_{\rm MM}}{z_{\rm RB}W_{\rm RB} + z_{\rm MM}W_{\rm MM}}\right) . \quad (3)$$

Generally, $z_{\rm RB} > 0$ and the rigid body torque $\tau_{\rm RB}$ provides a restoring moment that significantly contributes to the roll stability of the vehicle (at the cost of a decreased range of attainable roll angles). It is clear from (3) that a rectilinear moving mass will be limited in roll to some range $|\phi| < \pi/2$.

Now consider a cylindrical moving mass actuator design. Let the position of the mass be given in the body frame as $(r\cos\alpha, r\sin\alpha)$ where r is the distance of the moving mass from the center of the disk, and where α is the angle of the mass position measured clockwise from the $y_{\rm B}$ axis. Define the angle $\alpha' = \alpha - \phi$. The torque from the moving mass is then $\tau_{\rm MM} = r\cos\alpha' W_{\rm MM}$. By varying $\alpha' \in [0, 2\pi)$ the following range of equilibrium roll angles may be obtained:

$$\phi = \text{asin}\left(\frac{rW_{\rm MM}}{z_{\rm RB}W_{\rm RB}}\cos\alpha'\right) . \quad (4)$$

From (4) we find that the moving mass must be designed such that $rW_{\rm MM} \geq z_{\rm RB}W_{\rm RB}$ for the glider to the have unlimited roll control. However, if $z_{\rm RB} \neq 0$ then it is clear that the roll dynamics will be different in both upright ($\phi = 0$) and inverted orientations ($\phi = \pi$). (In one orientation $\tau_{\rm RB}$ may provide a restoring force, while in the other it will be destabilizing.) To mitigate this effect the glider should be trimmed such that $z_{\rm RB} = 0$. In our hypothetical example, $z_{\rm RB} = 0$ suggests that any nonzero $W_{\rm MM}$ could rotate the disk to a stable equilibrium point. However, in practice, $W_{\rm MM}$ must be large enough to rotate the glider in the presence of viscous damping moments. Further, $W_{\rm MM}$ must be large enough such that, in the absence of a restoring rigid body torque, it provides adequate roll stability in the presence of disturbances.

It is preferable for a shallow water glider with unlimited roll control to "flip over" on the surface, when transitioning from an ascent to a descent, rather than while it is underway. This maximizes the time available for the glider to maintain a steady glide. However, there are several challenges associated with flipping over on the surface. As the glider begins to roll its wings on the surface there is a discontinuous change in buoyancy as one wing leaves the water. The result is that the buoyancy of the other (submerged) wing is not balanced and therefore a roll moment acts to restore the vehicle to the level orientation (see Fig. 9). This restoring moment can be significant since the moment arm of the wings' center of buoyancy is typically several times that of the moving mass. The *VTUG* initially employed cambered wings, however we found that these were too buoyant and prevented the vehicle from rolling on the surface. Replacing these with flat plate steel wings greatly improved the roll performance.

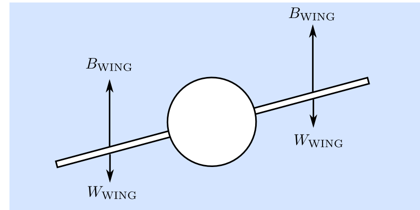

(a) At depth the wings are submerged and do not induce a rolling moment

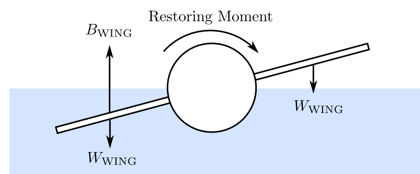

(b) On the surface there is a discontinuous change in wing buoyancy causing a restoring moment that works to keep the glider level

Fig. 9: Effect of wing buoyancy on rolling moments

Another factor that was found to affect the ability of the glider to roll was the drag due to wind acting on the wings. A wing extending straight above the water has a relatively large surface area and the resulting drag forces may be signficant. On calm days it was observed that by rolling clockwise, or counter-clockwise, the wings would act as paddles to change the heading of the vehicle. This effect may be exploited to re-orient the glider prior to initiating a dive.

IV. Acoustic Long-Baseline Positioning System

To position the glider while it is underway, an acoustic long-baseline (LBL) ranging system was developed [7]. The system consists of three mobile acoustic buoys (see Fig. 1(b)) equipped with GPS units, radios, acoustic transducers and micro-modems from Woods Hole Oceanographic Institute (WHOI). When deployed the buoys were anchored to the floor of the lake and their acoustic transducers were held mid-water at equal depths. The glider was programmed to ping the buoys in succession with a 5 s interval between pings (resulting in a 15 s ranging cycle). If the buoys received the ping (not always the case) they would return an acknowledgment (containing clock information). The micro-modem on board the glider calculated the time-of-flight corresponding to each successful ping. Refer to [7] for the electrical, mechanical, and software design of the LBL system.

A. Depth Placement of LBL Transducers

An experiment was conducted to determine the optimal depth to which the acoustic buoys' transducers should be deployed. Since the speed of sound profile and acoustic properties of the operating environment were not well known the optimal placement was determined experimentally. A test was conducted with the glider transducer removed from the vehicle and connected to a fourth 25 m wet-mateable cable. The depth d of the buoys' transducers was incrementally varied from: 5 m, 10 m, 15 m, to 20 m. For each configuration the glider transducer was also lowered to a series of depths (1 m, 5 m, 10 m, 15 m, or 20 m) for 5 minutes respectively. The test setup is shown in Fig. 10. The resulting percentage of successful pings (from each buoy) is given in Fig. 11. We found that the performance of the entire system was generally better when all of the transducers were at similar depths. This suggests that staggering the transducer depths may be a strategy to obtain successful pings at unique depths. However, for the purposes of localization, consecutive pings must be obtained from unique buoys and therefore the glider cannot simply ping the buoy at the nearest depth. Note that the ground station and glider transducer had low (even zero) ping success percentages when they were not at similar depths. As shown in Fig. 10, the ground station and glider transducers are both directly below the hull of the aluminum boat. We hypothesize that reverberations from the hull may have contributed to the poor performance in this case. The depth that gave the overall highest percentage of successful pings was 5 m and was chosen for our LBL system.

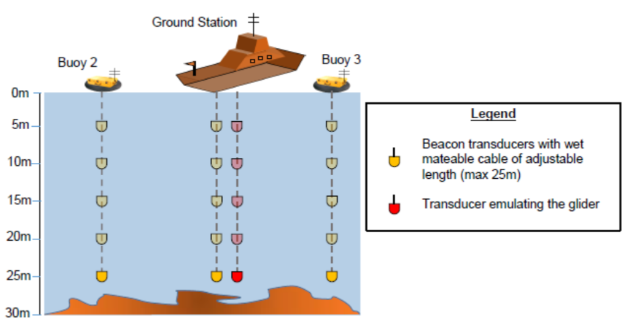

Fig. 10: Transducer depth placement test: for each fixed buoy transducer depth (yellow markers) the glider transducer (red marker) was incrementally lowered and the ping success percentage was recorded.

B. Planar Motion LBL Ranging Performance

The LBL ranging performance was tested in Claytor Lake, VA by traveling in a "lawn-mowing" type pattern in the vicinity of three buoys (denoted with large circular markers in Fig. 12(a)). A GPS-equipped boat was used to emulate the motion of the glider. The true path of the boat could then be compared to estimates based on range measurements. The locations of the pings on the track are shown in Fig. 12(a) with small colored circular markers that indicate the buoy from which the ping response originated. It is clear the ping success percentage for a given buoy varies spatially across the test site. The position estimates were obtained off-line using a static iterative nonlinear least squares estimator [8], and the Bancroft algorithm (originally developed for GPS positioning) [9] which provides a direct algebraic solution.

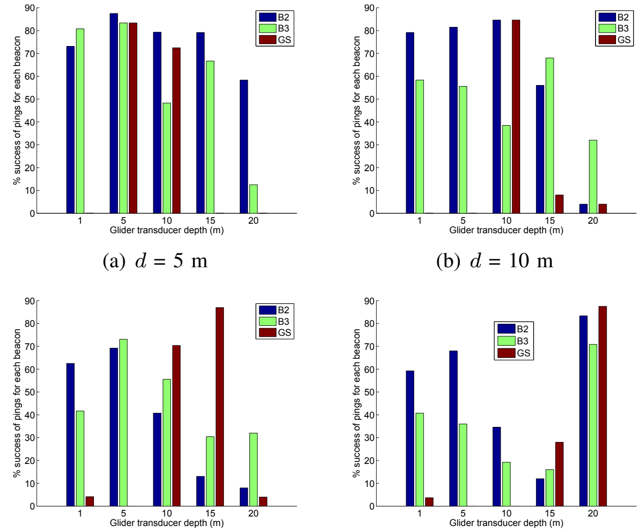

(a) d = 5 m (b) d = 10 m

(c) d = 15 m (d) d = 20 m

Fig. 11: Ping success percentage for various buoy transducer depths.

A planar position estimate could be calculated only when at least two consecutive range measurements were available. (See Fig. 12(a) with regions on the track where there are no estimates.) Fig. 12(c) shows a histogram of pings with and without a successful response from the buoys. The ping success percentages for all buoys were found to be similar. We observed similar performance at several other test sites on the lake. Ambient noise, multi-path from the rocky bottom, and strong temperature gradient of the shallow water lake may have contributed to the loss of pings.

V. Sawtooth Glide Experiments

Initial sawtooth tests were performed in a swimming pool. The glider employed a modified bladder that used a fabric covering to restrict expansion beyond some volume and allow higher pressures (up to 5 psi). This higher pressure bladder resulted in faster deflation rates and made the bladder less susceptible to small changes in ambient pressure (from pitch angle or depth changes). The data from a sawtooth pool test is given in Fig. 13. It is important to note that the pool is much too shallow for the glider to establish a steady glide and the sawtooth here consists of inefficient transient motions. The bladder pressure oscillated near the surface and further gain tuning was required. The target depth of the glider during the sawtooth (1.5 m) was overshot by about 1.5 m. Because of the limited depth of the swimming pool, the moving mass was limited in its range of motion. The descent and ascent pitch attitudes were about ± 60 deg.

Once the performance of the LBL system was verified, it was then deployed for position estimation of the glider while it performed sawtooth dives in Claytor Lake, VA. The test setup is shown in Fig. 14. The data in Fig. 15 shows the orientation, actuator commands and depth of the glider during

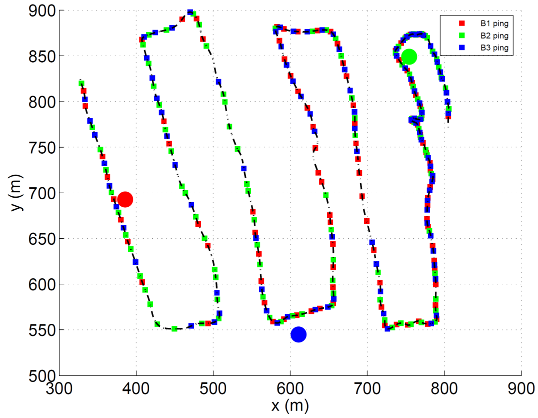

(a) Actual path of boat with superimposed successful ping locations

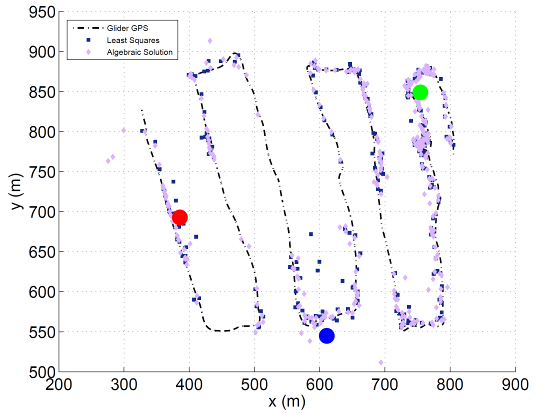

(b) Offline estimate of boat position based on range measurements

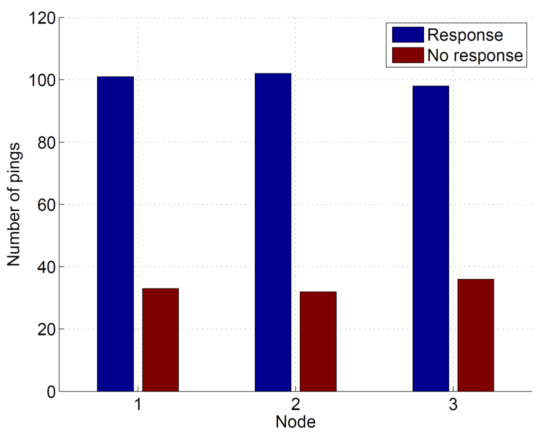

(c) Histogram of successful vs. unsuccessful range measurements

Fig. 12: Testing the LBL system with a GPS-equipped boat emulating the gliders motion

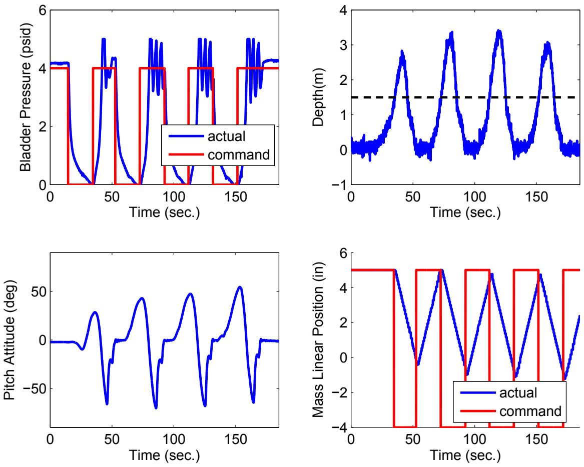

Fig. 13: Pool sawtooth test

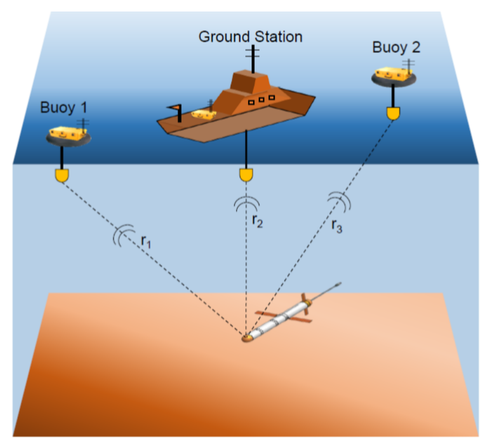

Fig. 14: LBL ranging with boat acting as a buoy

a representative sawtooth dive. The pitch attitude during the dive was much steeper than desired during both the ascent and descent. This is attributed to the numerous difficulties associated with trimming the vehicle that we have described in this paper. Although the glider was able to receive successful pings when it was stationary at the surface, the glider received no pings while it was underway. Thus LBL positioning could not be performed. During these LBL tests the nosecone was removed so that it does not attenuate the sound around the transducer. We believe that the lack of successful pings during the sawtooth dive may be a result of the following factors: a) as the glider descends and ascends the body of the glider may occlude the transducer located in the nose, b) the moving mass motors and solenoid valves introduce significant noise into the LBL system, especially during sawtooth dives when they are most active, and c) the bladder is regulated by exhausting air that forms numerous bubbles in the vicinity of the transducer that may cause scattering of sound. To test the first hypothesis regarding the mounting and orientation of the transducer we performed sawtooth dives again with the transducer moved from the nose to the hull (see Fig. 16) of the vehicle. No performance improvements were observed. Although most underwater gliders do not directly measure lateral position, enabling this functionality would support model identification, path following, and a range of other objectives.

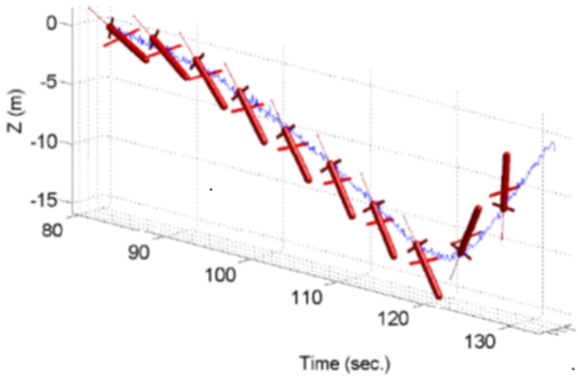

(a) Visualization of glider orientation for a sawtooth dive

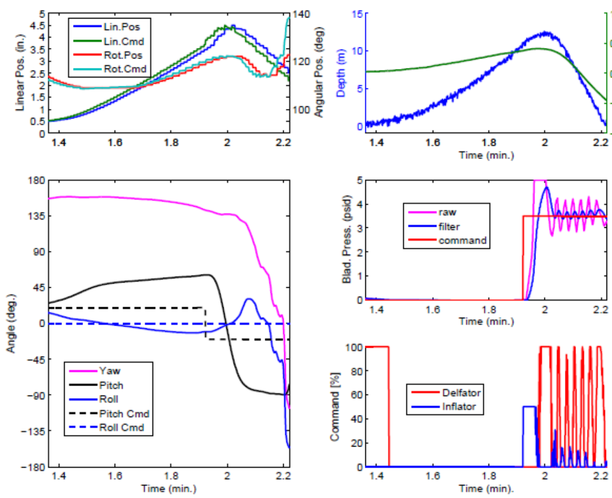

(b) Attitude data for the dive

Fig. 15: Sawtooth glide test with acoustic positioning and attitude control

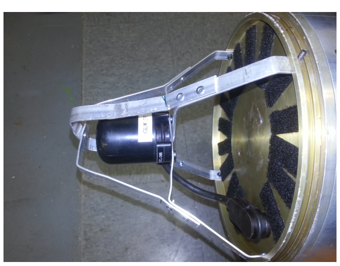

(a) Nose mounted

(b) Hull mounted

Fig. 16: Various mounting locations of the acoustic transducer

VI. Conclusion

In testing a novel underwater glider design and a long baseline ranging system in a shallow water lake, we identified several challenges associated with key glider systems that were designed to make the glider faster and more maneuverable. For example, a pneumatic buoyancy engine was found to generate large attitude disturbances that challenged the vehicle's attitude control system, a cylindrical moving mass actuator. Despite the challenges we encountered, the pneumatic buoyancy engine was able to reliably control the depth of the glider and provide large and rapid buoyancy changes. This type of buoyancy engine may be useful in applications requiring the vehicle to extract itself from a layer of debris after a prolonged period of being inactive on the sea-floor (e.g. if the vehicle were to passively collect measurements and periodically surface to transmit data). Field tests of the *Virginia Tech Underwater Glider* underscore the challenges involved in developing new motion control concepts. However, the experimental results also suggest that pneumatically powered glider may be an effective mobile sensing technology in shallow water and strong currents.

Acknolwedgments

The authors gratefully acknowledge the sponsorship of the Office of Naval Research under Grants No. N00014-08-1-0012, N00014-10-1-0022, and N00014-13-1-0060.

References

[1] A. Wolek and C. A. Woolsey. Feasible Dubins Paths in Presence of Unknown, Unsteady Velocity Disturbances. *Journal of Guidance, Control, and Dynamics*, 38(4):782–787, 2015.

[2] A. Wolek, E. M. Cliff, and C. A. Woolsey. Time-Optimal Path Planning for a Kinematic Car with Variable Speed Controls. in review, 2015.

[3] A. Wolek, E. M. Cliff, and C. A. Woolsey. Energy-Optimal Paths for a Glider with Speed and Load Factor Controls. *Journal of Guidance, Control, and Dynamics*, to appear, 2015.

[4] A. Wolek, J. Burns, C. A. Woolsey, J. Quenzer, L. Techy, and K. A. Morgansen. A Maneuverable, Pneumatic Underwater Glider. In *Proceedings of the 2012 IEEE OCEANS Conference and Exhibition*, Piscataway, NJ, 2012. IEEE.

[5] N. E. Leonard. Stability of a Bottom-heavy Underwater Vehicle. *Auotmatica*, 33(3):331–346, 1997.

[6] N. E. Leonard and J. G. Graver. Model-Based Feedback Control of Autonomous Underwater Gliders. *IEEE Journal of Oceanic Engineering*, 26(4):633–645, 2001.

[7] T. Gode. *Long Baseline Ranging Acoustic Positioning System*. Master's thesis, Virginia Polytechnic Institute and State University, Blacksburg, VA, 2015.

[8] L. Techy, K.A. Morgansen, and C.A. Woolsey. Long-Baseline Acoustic Localization of the Seaglider Underwater Glider. In *Proceedings of the 2011 American Control Conference*, Piscataway, NJ, 2011. IEEE.

[9] S. Bancroft. An Algebraic Solution of the GPS Equations. *IEEE Transactions on Aerospace and Elecrtrical Systems*, 21(7):56–59, 1985.